Phase diagram of a family of one-dimensional nearest-neighbor tight-binding models with an exact mobility edge*

Long-Yan Gong(巩龙延)[1,2,3,†] and Xiao-Xin Zhao(赵小新)[2]

[1] *Department of Applied Physics, Nanjing University of Posts and Telecommunications, Nanjing* 210003, *China*
[2] *Institute of Signal Processing and Transmission, Nanjing University of Posts and Telecommunications, Nanjing* 210003, *China*
[3] *National Laboratory of Solid State Microstructures, Nanjing University, Nanjing* 210093, *China*

(Received 17 February 2017; revised manuscript received 14 April 2017; published online 8 June 2017)

Recently, an interesting family of quasiperiodic models with exact mobility edges (MEs) has been proposed (*Phys. Rev. Lett.* **114** 146601 (2015)). It is self-dual under a generalized duality transformation. However, such transformation is not obvious to map extended (localized) states in the real space to localized (extended) ones in the Fourier space. Therefore, it needs more convictive evidences to confirm the existence of MEs. We use the second moment of wave functions, Shannon information entropies, and Lypanunov exponents to characterize the localization properties of the eigenstates, respectively. Furthermore, we obtain the phase diagram of the model. Our numerical results support the existing analytical findings.

Keywords: Anderson localization, quasiperiodic model, mobility edge

PACS: 72.20.Ee, 72.15.Rn, 71.23.An **DOI:** 10.1088/1674-1056/26/7/077202

1. Introduction

Since Anderson published his initial theoretical paper titled *Absence of Diffusion in Certain Random Lattices* in 1958,[1] disorder-induced localization, i.e., Anderson localization has become an important and fundamental concept in condensed matter physics and disordered systems.[2–7] For a lattice with periodic potential, one-electron states are plane waves multiplied by periodic functions. However, there is no simple answer for non-periodic systems. Therefore, the nature of an electron state, i.e., whether a state is extended, localized, or critical, is an essential problem in this field.[8]

For an uncorrelated disorder potential, there exist mobility edges (MEs) separating localized states from extended ones in three dimensional systems;[1,2] however, according to the scaling theory, all states are localized in one and two dimensional systems.[9] For one-dimensional (1D) systems, MEs exist in several models, e.g., the Soukoulis–Economou model with incommensurate potentials,[10] slowly varying potential ones,[11] random-dimer potential ones,[12] long-range correlated disordered potential ones,[13] and the Anderson model with long-range hopping.[14] However, there are no analytical results about MEs for these 1D models.

On the other hand, the Aubry–André model is a 1D one-band tight-binding model with an on-site cosine incommensurate modulation potential.[15] According to the duality theory, there is a self-duality point.[15] The corresponding duality transformation is a simple Fourier transformation, which maps extended (localized) states in position space to localized (extended) ones in momentum space. All states are extended, critical, or localized depending on the potential strength. In other words, there exists a "metal–insulator" transition at a critical strength of the modulation potential. However, there are no MEs in the model. Very recently, Ganeshan, Pixley, and Das Sarma proposed an interesting family of 1D quasiperiodic nearest-neighbor tight-binding models.[16] For simplicity and convenience, we call it the GPD model. There exist self-duality points under a generalized duality transformation. Based on the transformation, they obtained the analytical critical condition about MEs. However, the physical means of the generalized duality transformation are not as obvious as those in the the Aubry–André model, so they numerically confirmed their result with the inverse participation ratio (IPR) and the typical density of states (TDOS).

As is well known to all, the IPR and the TDOS are two possible indices to reflect the Anderson localization transition. However, there may exist some pitfalls.[17] For example, the critical IPR have been chosen to be 0.16, 0.20, or even 0.006 (see Ref. [18] and references therein), which depends on the system sizes and models. It means that there is no fixed critical value to distinguish localized states from delocalized ones. The TDOS is very sensitive to small values of the wave function amplitude on individual lattice sites. However, small values may occur due to localization, but they may also occur due to the reduction in amplitude of extended wave functions at sites where the magnitude of the potential is large.[19] Due to the absence of a clearly defined zero, the TDOS is not a reliable measure of localization. Therefore, more convictive evidences are needed for the GPD model. In fact, almost all numerical realizations may present inaccuracies, so some judicious techniques such as finite size analysis are often used.[20] However, ambiguities at times cannot be eliminated. There-

*Project supported by the National Natural Science Foundation of China (Grant Nos. 61475075 and 61170321).
†Corresponding author. E-mail: lygong@njupt.edu.cn
© 2017 Chinese Physical Society and IOP Publishing Ltd

fore, it is worthwhile using different quantities to confirm the analytical critical condition about MEs in the GPD model.

The second moment (SM) of wave functions is widely used to measure the extention of the wave function in space.[21,22] We have provided a method to distinguish delocalized, localized, or critical states with the help of comparisons of Shannon information entropies (SEs) in position space and that in momentum ones.[23] It is an efficient method even for small systems. For large systems, a numerically accurate renormalization scheme is an efficient method (see Ref. [20] and references therein). The energy-depended Lypanunov exponents (LEs) can well reflect the electronic localization properties. However, the localized states are difficult to distinguish from the gapped ones based on LEs. The renormalization scheme cannot determine the energy eigenstates, so it is not suitable to locate MEs. Fortunately, Persson has provided a simple efficient method to compute all the eigenvalues of a symmetric tridiagonal matrix for very large systems.[24] Combining the two aspects, we can locate MEs with LEs.

Based on the above considerations, we will numerically calculate the SMs, SEs, and LEs to understand the nature of eigenstates in the GPD model. The rest of the paper is organized as follows. In Section 2, we introduce the GPD model. In Section 3, we analyze the behaviors of SEs, SMs, and LEs in the GPD model, respectively. In Section 4, we summarize the results and draw our conclusions.

2. The Ganeshan–Pixley–Das Sarma model

A single electron in 1D lattice systems is considered. The family of tight-binding Hamiltonian is described by[16]

$$H=\sum_{n=1}^{N}V_n(\alpha,\phi)c_n^{\dagger}c_n+t\sum_{n=1}^{N}(c_n^{\dagger}c_{n+1}+\text{H.c.}), \tag{1}$$

where the on-site potential $V_n(\alpha,\phi)$ is characterized by the deformation parameter α and on-site potential strength λ, t is the nearest-neighbor hopping integral, $c_n^{\dagger}$ (c_n) is the creation (annihilation) operator of the n-th site, and N is the lattice size.

One family of the GPD model is specified by an on-site potential

$$V_n(\alpha,\phi)=2\lambda\frac{\cos(2\pi nb+\phi)}{1-\alpha\cos(2\pi nb+\phi)}. \tag{2}$$

The on-site potential is a smooth function of α in the open interval $(-1,1)$. Each value of α corresponds to a different tight-binding model. ϕ is the original phase, which is redundant in localization. For a quasiperiodic modulation, b is set to be irrational. For $\alpha=0$, the model is the well known Aubry–André model. There exist self-duality points under a generalized duality transformation.[16] Based on it, the analytical critical condition about MEs when $\alpha\in(-1,1)$ is obtained as

$$\alpha E_{\rm c}=2\text{sgn}(\lambda)(|t|-|\lambda|), \tag{3}$$

where $\text{sgn}(x)$ is the sign function.

3. Results

We will study SMs, SEs, and LEs in the GPD model. In calculations, the irrational number b in Eq. (1) is approximated by the ratio of successive Fibonacci numbers: $F_m=F_{m-1}+F_{m-2}$, with $F_0=F_1=1$. In this way, choosing $b=F_{m-1}/F_m$ and lattice size $N=F_m$, we can obtain the periodic approximant for the quasiperiodic potential. Without loss of generality, we choose $t=-1$. In the following, $\lambda=-0.9$ and $\alpha=-0.52$ are chosen as examples. According to Eq. (3), $E_{\rm c}=5/13$.

3.1. Second moment of a wave function

The SM of a wave function is defined as

$$M_{\rm S}=\frac{1}{N}\left[\sum_{n=1}^{N}n^2|\psi_n|^2-\left(\sum_{n=1}^{N}n|\psi_n|^2\right)^2\right]^{1/2}, \tag{4}$$

where ψ_n is the amplitude of the wave function at the n-th lattice site. It measures the extention of the wave function in the real space. For an ideal delocalized state in a 1D infinity potential well, $M_{\rm S}=1/\sqrt{12}=0.2886751\cdots$, which is a characteristic value of delocalized states.[21] For general delocalized states, the SM values are between 0.18 and 0.29; the other values correspond to localized states.[22]

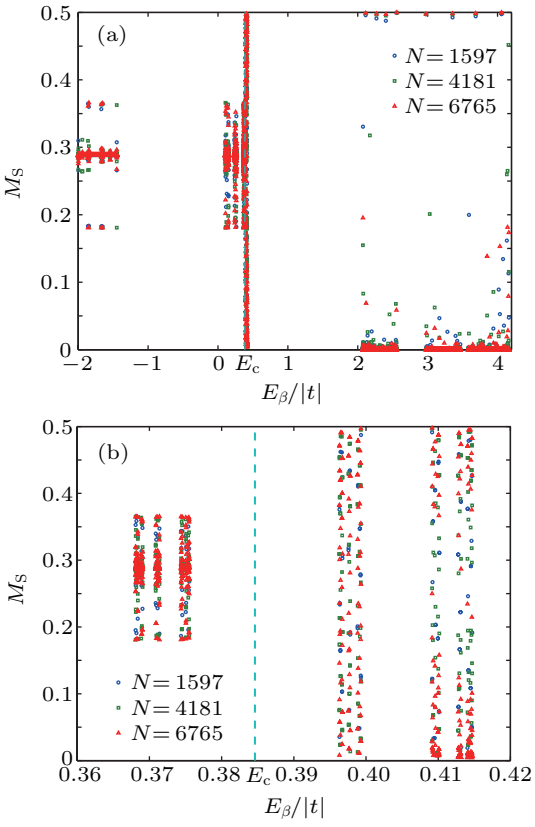


Fig. 1. (color online) The second moment versus eigenenergy E_β. (b) A partial enlarged view of panel (a) for eigenstates with E_β near $E_{\rm c}=5/13$. The vertical dashed line (cyan) denotes $E_\beta=E_{\rm c}$. Here, $\lambda=-0.9$, $\alpha=-0.52$, and the lattice size $N=1597,4181$, and 6765, respectively.

We plot the second moment versus eigenenergy E_β in Fig. 1 for lattice sizes $N = 1597, 4181$, and 6765, respectively. Figure 1(b) is a partial enlarged view of Fig. 1(a) for E_β near $E_c = 5/13$. For the three lattice sizes, $M_S \in (0.18, 0.37)$ and almost all M_S are in the region $(0.18, 0.29)$ for the eigenstates with $E_\beta < E_c$, while there are SEs with values near zero for the eigenstates with $E_\beta > E_c$. According to the above-mentioned criterion for M_S, they correspond to delocalized and localized states, respectively. In other words, E_c well separates delocalized states from localized ones. Therefore, it is a ME based on the localization properties of eigenstates reflected from SM.

3.2. Position- and momentum-space Shannon information entropies

The position-space SE for eigenstate $|\beta\rangle$ is defined by[23]

$$S_x = -\sum_{n=1}^{N} |\psi_n|^2 \ln(|\psi_n|^2). \tag{5}$$

Similarly, the momentum-space SE is

$$S_p = -\sum_{k=1}^{N} |\psi_k|^2 \ln(|\psi_k|^2). \tag{6}$$

Here $\psi_k = \frac{1}{\sqrt{N}} \sum_{n=1}^{N} \exp(-i2\pi nk/N)\psi_n$, $k = -[\frac{N}{2}], \ldots, [\frac{N-1}{2}]$, where $i^2 = -1$ and $[Z]$ is the integer part of Z. We define a reduced relative Shannon information entropy based on S_x and S_p, which is written as

$$S_R = (S_x - S_p)/(S_x + S_p). \tag{7}$$

For delocalized states, $S_R > 0$, while for localized states $S_R < 0$. The larger the S_R, the more delocalized the states are; the smaller the S_R, the more localized the states are. It is a simple method to discern the nature of the states.[23]

We plot the position- and momentum-space SEs S_x and S_p versus eigenenergy E_β in Fig. 2(a) for lattice sizes $N = 1597, 4181$, and 6765, respectively. For the three lattice sizes, S_x decreases as E_β increases, while S_p increases as E_β increases. Moreover, S_x is greater and smaller than S_p for $E_\beta < E_c$ and $E_\beta < E_c$, respectively. To see this, we plot S_R versus E_β in Fig. 2(b). At the same time, a partial enlarged view for E_β near $E_c = 5/13$ is plotted in Fig. 1(c). It clearly shows that S_R is positive and negative for $E_\beta < E_c$ and $E_\beta < E_c$, respectively. At a fixed E_β, for E_β smaller (larger) E_c, the larger the N is, the larger (smaller) the S_R is. According to the criterion for S_R just mentioned , they correspond to delocalized and localized states, respectively. Therefore, based on S_R, E_c is a ME.

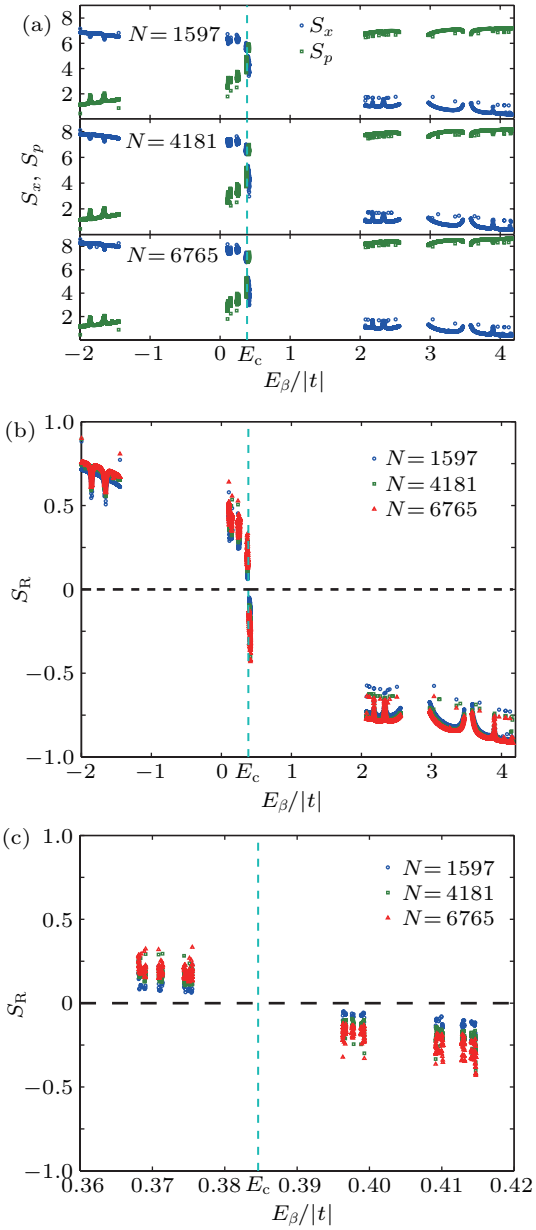


Fig. 2. (color online) (a) S_x (blue) and S_p (green) versus eigenenergy E_β, respectively. (b) S_R versus E_β. (c) A partial enlarged view of panel (b) for eigenstates with E_β near $E_c = 5/13$. The vertical dashed line (cyan) denotes $E_\beta = E_c$ and the horizontal dashed ones (black) denote $S_R = 0$. Here, $\lambda = -0.9$, $\alpha = -0.52$, and the lattice size $N = 1597, 4181$, and 6765, respectively.

3.3. Lypanunov exponent

The LE can be defined by

$$\gamma(E) = -\lim_{N\to\infty} \left(\frac{1}{N} \ln \left| \frac{G_{NN}(E)}{G_{0N}(E)} \right| \right), \tag{8}$$

where G_{0N} and G_{NN} are the Green-function matrix elements. We will use a numerically accurate renormalization scheme to obtain LEs.[20] The LE is determined by the relation

$$\gamma(E) = -\lim_{N\to\infty} \left(\frac{1}{N} \ln |t_{0N}^{\text{eff}}(E)| \right), \tag{9}$$

where t_{0N}^{eff} is the effective hopping integral between sites 0 and N when all the internal sites between them are properly decimated. The detail can be found in Ref. [20]. In numerical

calculations, we first compute all the eigenenergies E_α of the Hamiltonian in Eq. (1) for larger lattice sizes N with codes written by Persson.[24] We then use the numerically accurate renormalization scheme to calculate γ at energies E_α.

We plot γ versus eigenenergy E_β in Fig. 3(a) for the lattice sizes $N = 10946, 28657$, and 196418, respectively. A partial enlarged view of γ versus E_β for E_β near E_c is given in Fig. 3(b). They show that γ abruptly changes as E_β is near E_c. Almost all γ are near 0 for $E_\beta < E_c$, while γ is greater than 0 for $E_\beta > E_c$. They also show that for $E_\beta < E_c$, the larger N is, the less γ is, while for $E_\beta > E_c$, the larger N is, the larger γ is. It is known that γ approaches to 0 when the state is extended, while γ is finite when the state is localized.[20] Therefore, E_c is a ME.

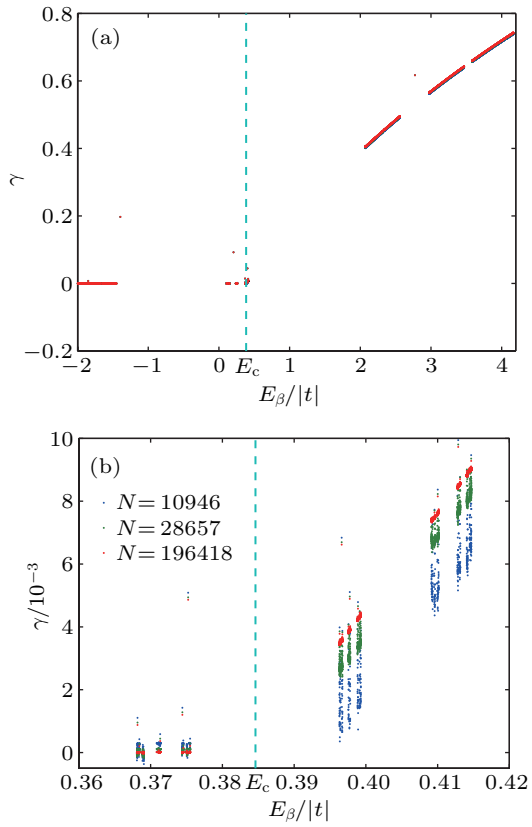


Fig. 3. (color online) (a) γ versus E_β. (b) A partial enlarged view of panel (a) for eigenstates with E_β near $E_c = 5/13$. The vertical line (cyan) denotes $E_\beta = E_c$. Here, $\lambda = -0.9$, $\alpha = -0.52$, and the lattice size $N = 10946$ (green), 28657 (blue), and 196418 (red), respectively.

3.4. Phase diagram

We have calculated SMs, SEs, and LEs at other α in the region $(-1, 1)$ and found that all our results support the analytical finding about E_c given in Eq. (3). We plot the phase diagram in Fig. 4. Here, the lattice size $N = 196418$ is used as an example. For larger lattice sizes, the results are similar. The energy-band $[E_{\min}, E_{\max}]$ is obtained with codes written by Persson.[24] In region I where $E_{\min} < E_c < E_{\max}$, MEs exist and they separate localized states from extended ones. In region II, $E_c > E_{\max}$ and all states are extended. In region III, $E_c < E_{\min}$ and all states are localized. In other words, in region I, local ME exists in the middle of the band, while in regions II and III, global ME exists beyond the band. At the bicritical point $(\alpha, \lambda) = (0, -1)$, it becomes the Aubry–André model and all states are critical. From Eq. (2), on-site potential $V_n(\alpha, -\lambda) = -V_n(\alpha, \lambda)$ and $V_n(-\alpha, \lambda) = -V_{n+F_m/2}(\alpha, \lambda)$. Therefore, the phase diagram for $\alpha \in [0, 1)$ can be easily obtained based on the symmetry of the potential.

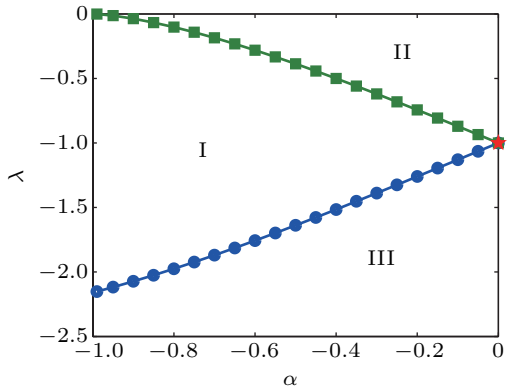


Fig. 4. (color online) Phase diagram for $\alpha \in (-1.0, 0]$. In region I , there are MEs separating localized states from extended ones. In regions II and III, all states are extended and localized, respectively. At the bicritical point (red star), all states are critical.

4. Discussion and conclusion

The GPD model is an interesting family of one-dimensional quasiperiodic nearest-neighbor tight-binding models. It has exact MEs. With the help of SMs, SEs, and LEs, we numerically studied the nature of eigenstates in the model. We found that the localization properties of the eigenstates reflected from these quantities are in excellent quantitative agreement with MEs. We gave the phase diagram. These studies provided further convictive evidence to support existing analytical findings.

References

[1] Anderson P W 1958 *Phys. Rev.* **109** 1492
[2] E. Abrahams (Ed.) 2010 *50 Years of Anderson Localization* (Singapore: World Scientific)
[3] Evers F and Mirlin A D 2008 *Rev. Mod. Phys.* **80** 1355
[4] Zhu H J and Xiong S J 2010 *Chin. Phys. B* **19** 037107
[5] Gong L Y and Tong P Q 2008 *Chin. Phys. B* **17** 0674
[6] Liao J, Shi G, Liu N, and Li Y Q 2016 *Chin. Phys. B* **25** 117201
[7] Chou C and Ho C 2014 *Chin. Phys. B* **23** 110302
[8] Maciá E and Maciá E 2014 *ISRN Condens. Matter Phys.* **2014** 165943
[9] Abrahams E, Anderson P W, Licciardello D C and Ramakrishnan T V 1979 *Phys. Rev. Lett.* **42** 673
[10] Soukoulis C M and Economou E N 1982 *Phys. Rev. Lett.* **48** 1043
[11] Das Sarma S, He S and Xie X C 1988 *Phys. Rev. Lett.* **61** 2144
[12] Dunlap D H, Wu H L and Phillips P W 1990 *Phys. Rev. Lett.* **65** 88

[13] de Moura F A B F and Lyra M L 1998 *Phys. Rev. Lett.* **81** 3735
[14] Rodríguez A, Malyshev V A, Sierra G, Martín-Delgado M A, Rodríguez-Laguna J and Domínguez-Adame F 2003 *Phys. Rev. Lett.* **90** 027404
[15] Aubry S and André G 1980 *Ann. Isr. Phys. Soc.* **3** 133
[16] Ganeshan S, Pixley J H and Das Sarma S 2015 *Phys. Rev. Lett.* **114** 146601
[17] Gong L Y, Li W J, Zhao S M and Cheng W W 2016 *Phys. Lett. A* **380** 59
[18] Gibbons M K, Logan D E and Madden P A 1988 *Phys. Rev. B* **38** 7292
[19] Song Y, Atkinson W A and Wortis R 2007 *Phys. Rev. B* **76** 045105
[20] Farchioni R, Grosso G and Pastori Parravicini G 1992 *Phys. Rev. B* **45** 6383
[21] Zhou P Q, Fu X J, Lu C H, Guo Z Z and Liu Y Y 1996 *Z. Phys. B* **100** 321
[22] Johansson M and Riklund R 1991 *Phys. Rev. B* **43** 13468
[23] Gong L Y, Wei L, Zhao S M and Cheng W W 2012 *Phys. Rev. E* **86** 061122
[24] Persson P O *Eigenvalues of tridiagonal matrices in matlab*